MASS SPECTROMETRIC CHARACTERIZATION OF HIGH-VALENT METAL-OXO, -PEROXO AND -PEROXY INTERMEDIATES OF RELEVANCE IN OXIDATION PROCESSES

Olga Bortolini[1]* and Valeria Conte[2]

[1]*Dipartimento di Chimica, Università della Calabria, Via Bucci 12 C, 87036 Rende (CS) Italy*

[2]*Dipartimento di Scienze e Tecnologie Chimiche, Università di Roma "Tor Vergata", Via della Ricerca Scientifica, 00133 Roma, Italy*

Received 26 October 2005; accepted 5 December 2005

Published online 7 March 2006 in Wiley InterScience (www.interscience.wiley.com) DOI 10.1002/mas.20085

The coupling of mass spectrometry with ionization techniques like electrospray ionization (ESI) or matrix-assisted matrix-assisted laser desorption-ionization (MALDI) offers many advantages over other well-established spectroscopic techniques employed for the investigation of intermediates or short-lived species in condensed-phase. In this review we describe some of the applications of mass spectrometry, in particular of ESI-MS to the detection and characterization of high-valent metal-oxo, -peroxo and -peroxy derivatives, crucial intermediates in the oxyfunctionalization of organic substrates. In addition, by utilizing gas-phase ion-molecule reactions and MS/MS experiments, information on the intrinsic reactivity of the short-lived intermediates may be obtained. The combined use of ESI-MS in association with other spectroscopic techniques and theoretical calculations is discussed as well. © 2006 Wiley Periodicals, Inc., Mass Spec Rev 25:724–740, 2006

Keywords: *reaction intermediates; oxidation processes; metal-oxo; metal-peroxo; metal-peroxy; mass spectrometry; ESI; MALDI*

I. INTRODUCTION

From its introduction in the mid-1980s, largely by Fenn and co-workers (Aleksandrov et al., 1984; Yamashita & Fenn, 1984), electrospray ionization mass spectrometry (ESI-MS) has been used to investigate a wide range of compounds including proteins, nucleotides, fullerenes, synthetic polymers, inorganic and transition-metal complexes (Fenn et al., 1990; Cole, 1997). Applications of ESI-MS to inorganic and organometallic chemistry have been discussed in two major and comprehensive reviews (Colton, D'Agostino, & Traeger, 1995; Henderson, Nicholson, & McCaffrey, 1998), together with others of more limited scope (Traeger & Colton, 1998; Henderson & Evans, 1999; Traeger, 2000; Plattner, 2001, 2003). Of particular interest are the accounts dealing with the identification and speciation of the short-lived intermediates of important catalytic cycles, formed in solution and transferred into the gas-phase by electrospray ionization. In this frame, ESI-MS is emerging as a diagnostic technique, which provides a powerful alternative to low-temperature NMR spectroscopy (Bonchio et al., 1999). Analytical applications of ESI-MS to transition-metal chemistry may be broadly divided into two categories: (i) the mass spectrometric characterization of well-defined species originally present in solution and transferred in the gas-phase, and (ii) the identification of transition-metal intermediates playing a crucial role in selected reactions, that is, oxidation, C–H activation, or olefin oligomerization, often in combination with other spectroscopic techniques like NMR, IR, UV-vis, and theoretical calculations (Conte & Bortolini, 2006).

Central to the field of homogeneous catalysis is the discovery that transition-metal systems are able to mediate organic reactions with high efficiency and selectivity. As far as oxyfunctionalization reactions of organic and inorganic substrates are concerned, these may be selectively achieved, generally in mild conditions with good yields, by means of oxidation reactions carried out by organic peracids (RCO–OOH), hydrogen peroxide H_2O_2, and alkyl hydroperoxides (ROOH), although only organic peracids are of synthetic interest because of their much higher reactivity in comparison with that of other peroxidic species. H_2O_2 and alkyl hydroperoxides are, in fact, quite weak oxidants, so to be synthetically attractive, they need to be activated. The most used catalysts are derivatives of some transition, metal ions, being the species included in the 4–7 groups, that is, Ti, V, Cr, Mo, W, and Re, very active (Conte & Bortolini, 2006). The accepted mechanistic scheme for metal-catalyzed oxidations with peroxides is sketched in Scheme 1. The features of the active oxidant depend on the nature of the oxygen donor and on its interaction with the metal precursor. In several examples, high-valent peroxometal species have been recognized as competent intermediates.

As far as the structure of the active complexes is concerned, both in the solid state and/or in solution, several pieces of evidence indicate that most of them share a η^2 triangular arrangement of the peroxo moiety around the metal center (Scheme 2). It has to be noted that coordination to the metal center of more than one peroxidic moiety is also possible. O_2^{2-} ligand can bind two metals in bimetallic μ-peroxo complexes in a variety of coordination modes.

In contrast, for other catalysts, like manganese or chromium, an oxo-metal species regulates the oxidation in the place of a peroxide functionality (Adam et al., 2002).

**Correspondence to:* Olga Bortolini, Dipartimento di Chimica, Università della Calabria, Via Bucci 12 C, 87036 Rende (CS) Italy. E-mail: o.bortolini@unical.it

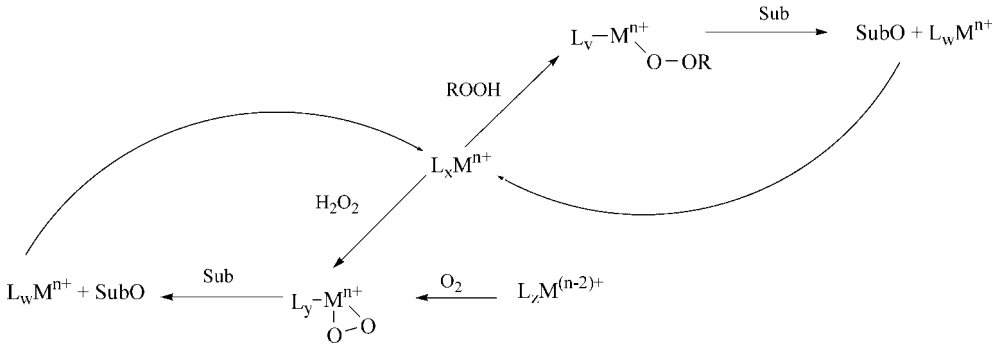

SCHEME 1

In this review, we will describe some of the applications of mass spectrometry, in particular of ESI-MS to the detection and characterization of high-valent metal-oxo, -peroxo, and -peroxy derivatives, crucial intermediates in the oxyfunctionalization of organic substrates. In addition, by utilizing gas-phase ion-molecule reactions and MS/MS experiments (Busch, Glish, & McLuckey, 1988) including collision-induced dissociations, information on the intrinsic reactivity of the short-lived intermediates may be obtained. The combined use of ESI-MS in association with other spectroscopic techniques and theoretical calculations will be discussed as well.

II. METAL-PEROXO

The case of vanadium peroxo derivatives is very instructive, in fact with this metal, the combined use of ESI-MS and ^{51}V-NMR, with the additional support of *ab initio* calculations, has been demonstrated as a powerful tool for obtaining direct information on the structure and the chemistry of the diverse peroxo vanadates formed in solutions upon addition of hydrogen peroxide to appropriate vanadium precursors (Bortolini et al., 1998, 1999, 2003; Conte et al., 2000; Bonchio et al., 2001a).

Vanadium (V) in aqueous solution is present as different vanadates species depending on pH and reduction potential (Crans et al., 2004). The ESI-MS analysis of vanadates solutions was conducted in mixed water–alcohol solvent, both in positive- (Bortolini et al., 1998; Walanda et al., 1999) and negative-ion mode (Bonchio et al., 2001b), thus mimicking acid and basic medium conditions (Cole, 1997). As far as monomeric cations are concerned, species such as $[OV(OX)_3H]^+$, with X = H or CH_3, were identified even though the most abundant peaks could be associated to dimeric species $[OV–O–VO(OH)_4H]^+$ and $[OV–O–VO(OCH_3)_3(H_2O)(OH)H]^+$. In negative-ion mode, where species formed are likely those found in neutral and basic media, primarily monomeric vanadium oxyanions were observed: $[VO_2(OY)_2]^-$ (Y = H, alkyl group) (Bortolini & Conte, 2005). In the presence of hydrogen peroxide, depending on the ratio V/peroxide and on pH value, diverse peroxo vanadates are formed in solutions and have been investigated. (Bortolini et al., 1998, 1999, 2003; Conte et al., 2000; Bonchio et al., 2001a,b). The first equilibrium depicted in Scheme 3 has been carefully analyzed with positive-ion mode mass spectra of acid H_2O/CH_3OH solutions containing equimolar amount of vanadium precursor and hydrogen peroxide. Most of the peaks identified in the spectrum (Bortolini & Conte, 2005) correspond to monoperoxo derivatives $[OV(O_2)(H_2O)_m(MeOH)_n]^+$ bearing dissimilar coordination sphere composition (m, $n = 0–4$) that is $[OV(O)_2]^+$ *m/z* 99, $[OV(O)_2(H_2O)]^+$ *m/z* 117, $[OV(O)_2(MeOH)]^+$ *m/z* 131, $[OV(O)_2(H_2O)_2]^+$ *m/z* 135, $[OV(O)_2(H_2O)(MeOH)]^+$ *m/z* 147. Very interesting is the observation that in the spectrum, there is still the presence of the ionic species at *m/z* 83, identified as VO_2^+. This experimental evidence indicates VO_2^+ as precursor for the formation of peroxo derivatives, according to Equation (1) in Scheme 3.

Monoperoxo species with one solvent molecule coordinated to vanadium are the most abundant ions observed. If these ions, upon isolation in the ion trap, are allowed to interact with neutral solvent molecules, that is, water or methanol, in low pressure condition, the reactions observed are: (i) exchange, in the coordination sphere, between water and methanol; (ii) coordination of a second molecule of solvent (Bortolini et al., 1998), (Scheme 4).

These findings clearly demonstrate that substitution of water molecules with methanol and vice versa in the coordination

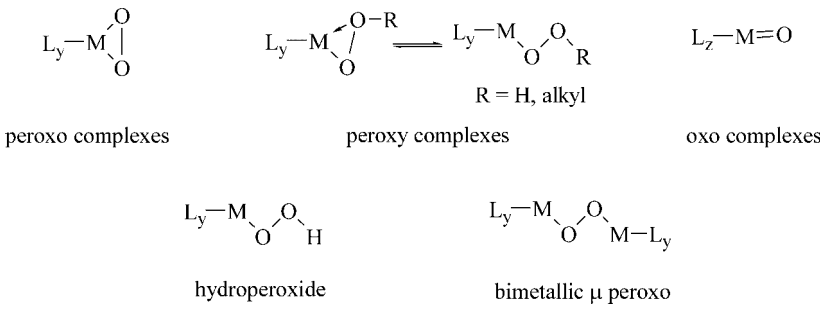

SCHEME 2.

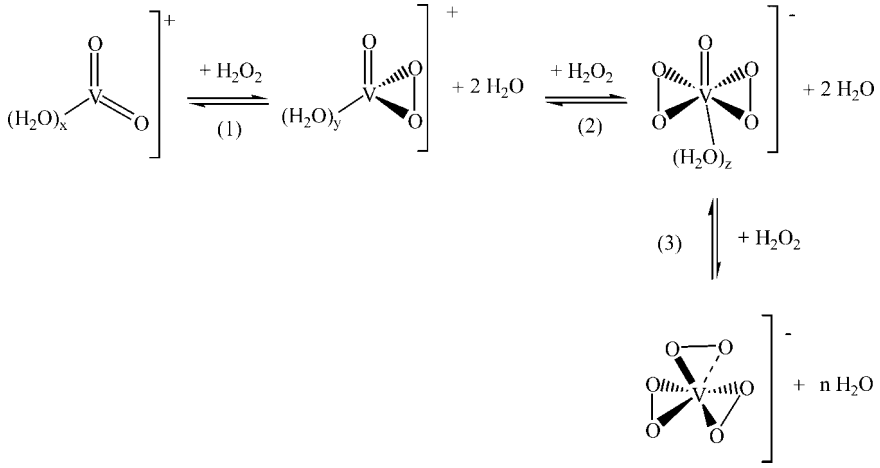

SCHEME 3.

sphere of monoperoxo vanadium complexes is a conceivable and detectable process in gas-phase. Its viability in solution has been verified with ^{51}V NMR spectra (Bortolini et al., 1998). Such exchange processes between water and methanol have also been studied by *ab initio* calculations carried out on addition reactions to the "naked" ion $[OV(O)_2]^+$ of either H_2O or MeOH molecule (Bortolini et al., 1998).

Monoperoxo vanadium species have been also invoked as active intermediate in functional mimicking system for vanadium-dependent bromo-peroxidases enzymes (Bortolini & Conte, 2005 and refs cited therein), in particular, in a vanadium-based two-phase procedure for bromination and oxybromination of aromatic and unsaturated organic substrates (Bortolini et al., 2003 and refs cited therein). In such a system, an intermediate of the type $[OV(OH)(OBr)(H_2O)n]^+$, derived from oxidation of bromide by a monoperoxo vanadium complex, was postulated. To gain direct verification on the occurrence, composition, and structure of such "bromine equivalent" intermediate, the $V/H_2O_2/H^+$ system was further investigated

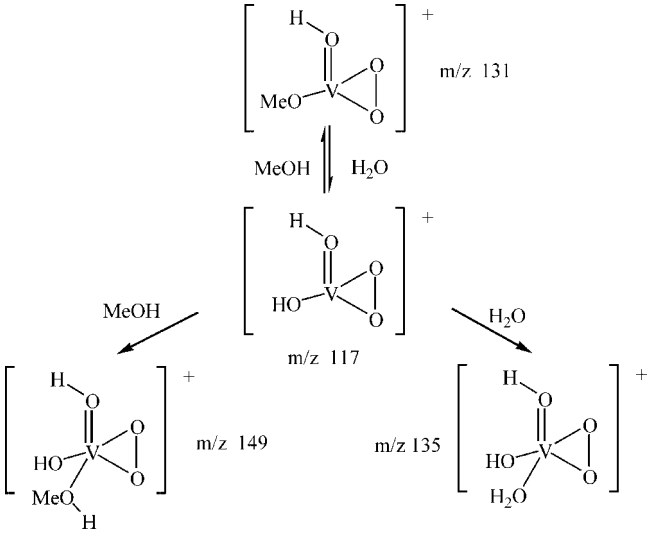

SCHEME 4.

by ESI-MS analysis, using a mixed water–methanol infusion solvent (Bortolini et al., 2003). The addition of Br^-, to the previous mixture, produced major changes into the positive-ion mode mass spectra, which basically consisted of $[OV(O_2)(H_2O)_m(MeOH)_n]^+$ ions. Indeed, formation of new vanadium species containing a single bromine atom was observed. On the basis of isotopic cluster analysis and MS^n spectra, the formal structure of those species has been anticipated as indicated below in Scheme 5.

The spectrometric evidence obtained was of fundamental importance for supporting, together with theoretical calculation and experimental studies, the formation of the V-containing bromine equivalent species in the catalytic cycle cited above (Bortolini et al., 2003).

Monoperoxo derivatives were also analyzed in negative-ion mode. As already indicated above, in "alkaline medium" and in the absence of hydrogen peroxide, V(V) exists primarily as monomeric oxyanions (VO_4^{3-}, HVO_4^{2-}, $H_2VO_4^-$). The negative-ion mode mass spectrum, observed after the addition of H_2O_2 (equimolar to V(V)) and obtained in H_2O–Pr^iOH as infusion solvent, showed the presence of two ionic species centered at *m/z* 201 and 217. The first one corresponds to $[O_2V(OPr^i)_2]^-$, whereas the second peak was attributed to the monoperoxo complex $[OV(O_2)(OPr^i)_2]^-$ with the help of MS^2 and ^{17}O labeling experiments, (Scheme 6).

Very interestingly, the MS^2 spectra, obtained upon selection of the $[OV(O_2)(OPr^i)_2]^-$ species, showed a fragmentation pattern mainly consisting of a 58-Da fragment expulsion, which formally corresponds to the release of C_3H_6O, that is, an acetone molecule. Monoperoxo vanadium compounds are in fact known to oxidize primary and secondary alcohols to carbonyl derivatives with the parallel reduction of molecular oxygen to H_2O_2 (Bonchio et al., 2001b). In the specific case, ESI-MS spectra directly observe the oxidation of Pr^iOH to acetone in agreement with literature reports (Bonchio et al., 2000).

According to the equilibria reported in Scheme 3, the increase of the concentration of hydrogen peroxide, as well as the increase of pH, causes the formation of diperoxo vanadates. These complexes have thus been studied by using ESI-MS in negative-ion detection mode. The spectra obtained show that most of the

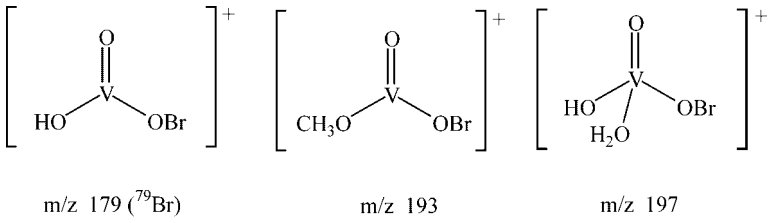

SCHEME 5.

observed peaks can be easily ascribed to V(V) diperoxo compounds containing water and/or alcohol solvent molecules in the coordination sphere $[OV(O_2)_2(H_2O)_m(ROH)_n]^-$. Interestingly, the naked ion $[OV(O_2)_2]^-$ appears to be the most abundant ionic species in agreement with speciation data obtained in solution (Andersson et al., 2000). When this ion is mass selected and submitted to collision-induced fragmentation (MS^2), the decomposition of both peroxo bridges is observed (32-Da loss) with formation of vanadate or solvent containing vanadate ions $[VO_3(H_2O)_m(ROH)_n]^-$. Coordination of one or two ligands (L) either solvent molecules (H_2O, ROH) or specific molecules like histidine, pyridine etc., to $[OV(O_2)_2]^-$ is a favorable process observed both in solution and in gas-phase (Bortolini et al., 1999; Andersson et al., 2000; Conte et al., 2000). Of particular interest, in this context, are the studies carried out by ESI-MS on the coordination of histidine and histidine-like ligands to the diperoxo derivative, (Scheme 7).

Nitrogen-containing ligands bind vanadium peroxo derivatives with a known and facile process. Furthermore, the choice of the ligands indicated in Scheme 7 has been recommended on the basis of the structure of vanadium-containing haloperoxidases enzymes which present histidine residues coordinated to the metal through imidazole N-epsilon aromatic nitrogen (Messerschmidt, Prade, & Wever, 1997). Coordination of one or two ligands to the metal center has been observed and the corresponding peroxidic species $[VO(O_2)_2L]^-$ and $[VO(O_2)_2L_2]^-$ species have been characterized. In particular, with MS^2 experiments, specific fragmentations of the peroxidic moiety were distinguished as a function of the nature and the number of the ligands, see Scheme 7. In particular, the vanadium diperoxo compounds containing one heteroligand in the coordination sphere generally release a 32-Da fragment *via* decomposition of both peroxidic bridges, on the other hand, in the presence of two ligands, expulsion of a 34-Da fragment is observed when a free carboxylic function is present in the framework of the ligand itself. These peculiar fragmentations allowed, *inter alia*, to obtain further evidence on the occurrence of the protonation of the peroxidic moiety as a crucial step in the activation of vanadium peroxo compounds (Bortolini et al., 1999). This step has biochemical implication in the reactivity of vanadium haloperoxidases enzymes. In fact, by using ^{17}O-NMR and enriched ^{17}O-H_2O_2, signals ascribable to a hydroperoxidic form of *Ascophillum nodosum* bromoperoxidase enzyme have been detected (Čsny et al., 2000).

The step-by-step addition of H_2O_2 ($\geq$50 equivalents with respect to V(V)) progressively converts the diperoxo species into the triperoxo derivative, according to Equation (3) in Scheme 3. The negative-ion mode ESI mass spectra of solutions containing large excess of hydrogen peroxide (from 50 to 200) in Pr^iOH-0.5 mol/L H_2O, are characterized by the presence of two major ions at *m/z* 131 and 147, respectively. Less intense, but equally important, ionic species are found at *m/z* 99, 115, 133, 149, and 165. For relatively low excesses of H_2O_2 over V(V) (50–150 equivalents), the *m/z* 131 ion, corresponding to the oxo-diperoxo derivative (Bortolini et al., 1999), is dominant; however, a progressive overtake performed by the species centered at *m/z* 147 is observed as the hydrogen peroxide concentration is increased. By analogy with previous studies, carried out using either ethanol or Pr^iOH as mobile phases, the system under investigation was studied in both alcoholic solvents showing no significant dependence from the carrier. The peroxidic species were identified on the basis of labeling experiments and MS^n

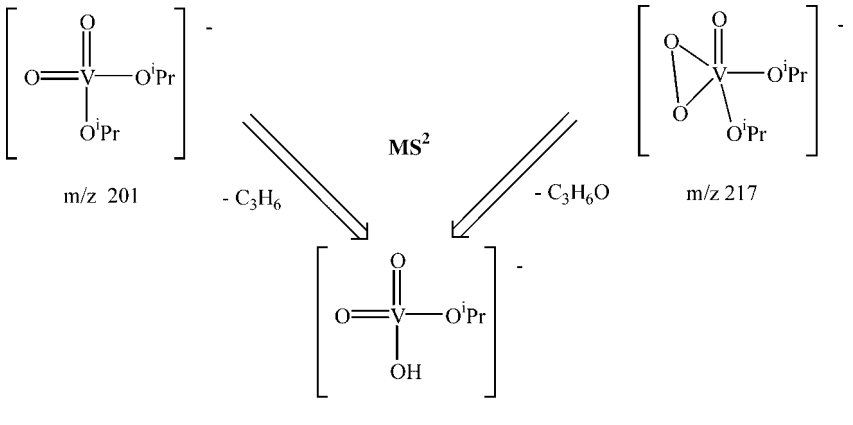

SCHEME 6.

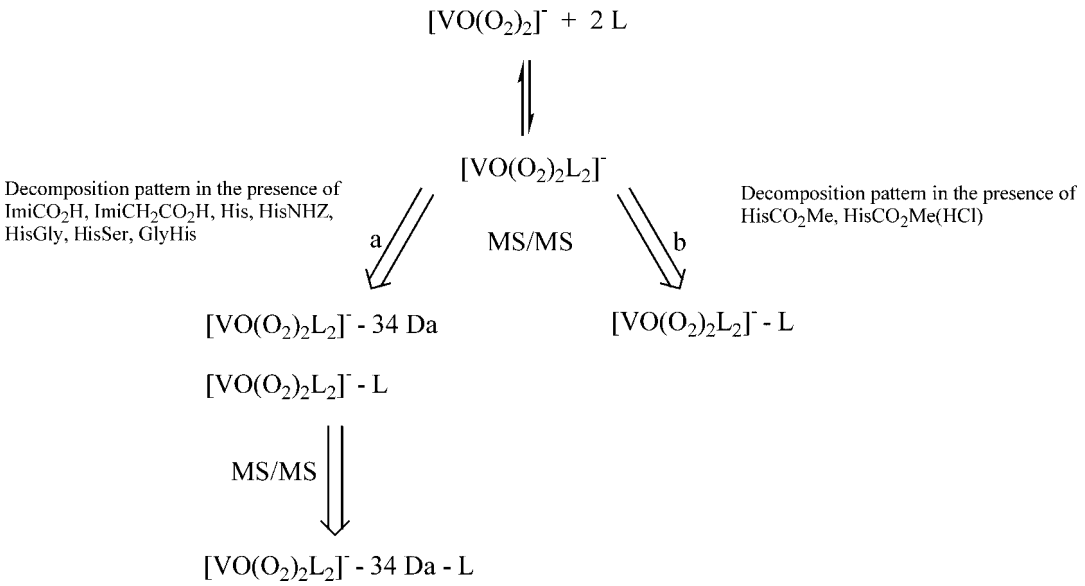

SCHEME 7.

spectra (Bortolini et al., 1998, 1999; Bonchio et al., 2001a). Among them, the species at *m/z* 147, identified as the vanadium triperoxo derivative $[V(O_2)_3]^-$, and that at *m/z* 115, assigned to the unprecedented dioxo monoperoxo compound $[O_2V(O_2)]^-$, are of particular interest. Labeling experiments were used to confirm this attribution. As expected, the replacement of water with $H_2{}^{17}O$ (ca. 50% isotope content) has no effect on the triperoxo anion, whereas formation of new peaks at *m/z* 116 and 117 is observed next to species at *m/z* 115. In agreement with literature data (Butler, Claugue, & Meister, 1994), this evidence indicates a fast exchange of the two oxo oxygens. When the triperoxo derivative is mass selected within the ion-trap analyzer and let to decompose by increasingly higher tickling voltages, the CID decompositions observed are the fragmentations of one and two of the three peroxidic bridges, thus affording the oxo diperoxo derivative $[OV(O_2)_2]^-$ *m/z* 131 and the dioxo monoperoxo derivative $[O_2V(O_2)]^-$ *m/z* 115, (Eq. (4) and Eq. (5) of Scheme 8, respectively) including its water and alcohol containing homologs $[O_2V(O_2)(ROH)]^-$, R=H, Et, Pr^i. The decomposition implicating two peroxo moieties is the most favorable pattern. This fragmentation is also the major decomposition observed with the oxo diperoxo derivative $[OV(O_2)_2]^-$, (Eq. (7) of Scheme 8). The direct decomposition of both peroxidic bridges, formally corresponding to the expulsion of an O_2 molecule, Equations (5) and (7), likely occurs through a two-step mechanism consisting of two subsequent oxygen atom losses. This figure has been demonstrated with experiments at increasing tickling energies.

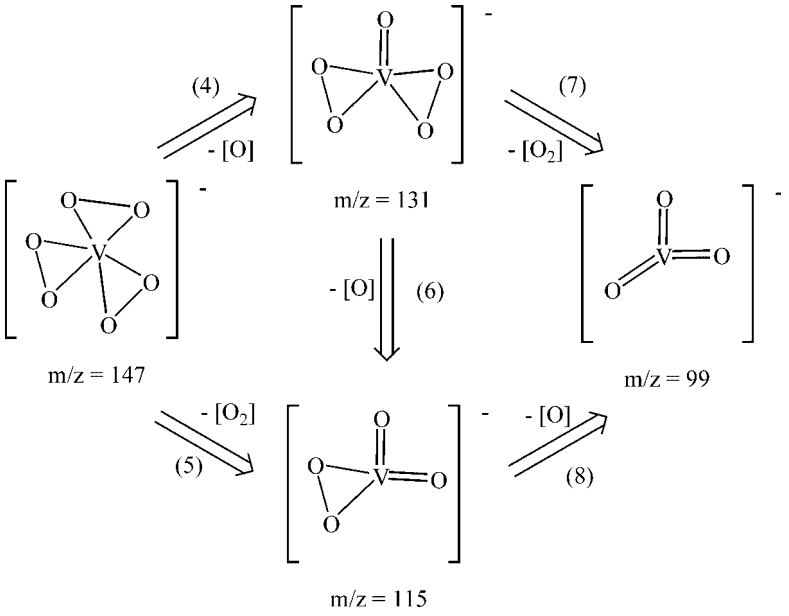

SCHEME 8.

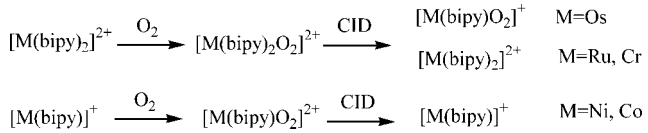

SCHEME 9.

Reactions of the *bis*(2,2′-bipyridine) ions $[M(bipy)_2]^{2+}$ with O_2 were investigated for M = Cr, Mn, Fe, Co, Ni, Cu, Ru, and Os, with the help of CID in MS/MS/MS experiments (Molina-Svendsen, Bojesen, & McKenzie, 1998). Doubly-charged dioxygen adducts $[M(bipy)_2O_2]^{2+}$ were observed for the Cr, Ru, and Os derivatives, whereas singly charged species $[M(bipy)O_2]^+$ were formed in the case of Co and Ni precursors. Except for the osmium derivative, formal release of O_2 was detected upon collision-induced dissociation experiments, (Scheme 9).

Despite the Os case, where the O–O bond seems to be broken, with both oxygen atoms independently bound to the osmium atom in an oxo fashion, M(IV)-peroxo or M(III)-superoxo complex ions are the most likely structures for these adducts.

A high-spin, five coordinated peroxo adduct of an iron^{II}–copper^{I} complex, obtained by reaction of $[(^6L)Fe^{II}Cu^{I}](BArF_{20})$ with O_2, has been recently characterized with the help of MALDI-TOF-MS (Ghiladi et al., 2005). Complex **1** is believed to have a relevant role in understanding the heme-copper dioxygen reactivity relevant to cytochrome-*c* oxidase O_2-reduction chemistry. The mass spectra of **1** were obtained by oxygenating $[(^6L)Fe^{II}Cu^{I}]^+$ with either $^{16}O_2$ or $^{18}O_2$ in CH_3CN at −40°C, followed by evaporation of the dioxygen adduct directly on the MALDI sample holder. In both cases, two peaks dominate the mass spectrum corresponding to ionic species at *m/z* 1,175 (*m/z* 1,177 when $^{18}O_2$ was used) identified as the μ-oxo complex $[(^6L)Fe^{III}–O–Cu^{II}]^+$ and to an ion at *m/z* 1,191 (*m/z* 1,195 when $^{18}O_2$ was used) assigned to the peroxo derivative **1**. A third, least intense, but isotopically sensitive peak at *m/z* 1,208 appeared in the mass spectrum not yet fully identified, but formally corresponding to $[(^6L)Fe^{II}Cu^{I}]^+$ with three additional oxygen atoms.

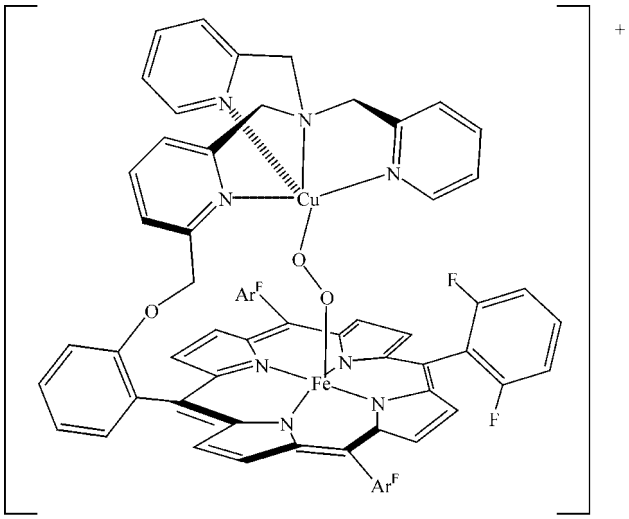

1 $[(^6L)Fe^{III}\text{-}(O_2)\text{-}Cu^{II}]^+$

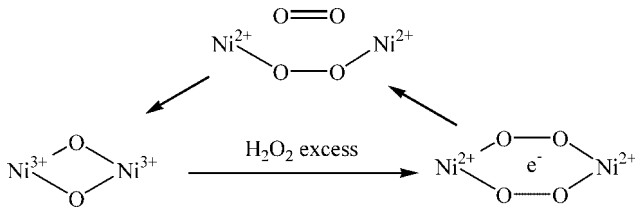

SCHEME 10.

A six-coordinate *bis*(μ-oxo)nickel(III) complex $[Ni_2(\mu\text{-}O)_2(Me_3\text{-}tpa)_2]^{2+}$ was synthesized by reaction of the *bis*-hydroxy derivative with H_2O_2. The ESI-MS analysis associated to this derivative showed the presence of an intense cluster at *m/z* 913 with the correct isotopic distribution for $[Ni_2(O)_2(Me_3\text{-}tpa)_2ClO_4]^+$ (Shiren et al., 2000). No incorporation of ^{18}O was observed if $H_2{}^{18}O_2$ was used, thus confirming a rapid exchange of the oxo groups by ^{16}O from water. Exposure of $[Ni_2(\mu\text{-}O)_2(Me_3\text{-}tpa)_2]^{2+}$ to large excess of H_2O_2 promotes the formation of the unprecedented reported μ-superoxo complex $[Ni_2(\mu\text{-}O_2)_2(Me_3\text{-}tpa)_2]^{2+}$ characterized by electrospray ionization as well. The related mass spectrum did not exhibit a signal at *m/z* 945 corresponding to $[Ni_2(\mu\text{-}O_2)_2(Me_3\text{-}tpa)_2ClO_4]^+$ but a signal at *m/z* 422 corresponding to the monomeric peroxo species $[Ni(O_2)(Me_3\text{-}tpa)]^+$ suggesting a disproportionation of the two coordinated superoxides to dioxygen and peroxide followed by the O–O bond scission of peroxide giving rise to $[Ni_2(\mu\text{-}O)_2(Me_3\text{-}tpa)_2]^{2+}$, according to Scheme 10.

III. METAL-PEROXY

A. Hydroperoxo

ESI-MS has been applied to the identification of the intermediate "activated bleomycin." The glycopeptide antibiotic bleomycin (BLM), reported to posses antineoplastic activity presumably related to its ability to bind iron and activate molecular oxygen thus forming "activated bleomycin," has been characterized as a hydroperoxo–Fe^{III} complex (Sam, Tang, & Peisach, 1994). Activated BLM may be formed both from Fe^{II}BLM and O_2 and by reacting Fe^{III}BLM with H_2O_2. The ESI mass spectrum of the mixture BLM and Fe^{III} affords, in addition to the signals ascribable to metal-free BLM, some new peaks identified as the doubly charged species $[Fe^{III} + BLM^+ – 2H^+]$ at *m/z* 734.3 and $[Fe^{III} + BLM^+ + OH^- - H^+]$ *m/z* 743.3. Addition of H_2O_2 gives rise to the formation of a new peak at *m/z* 751.3 proposed as $[Fe^{III} + BLM^+ + OOH^- - H^+]$, likely formulated as ferric peroxide BLM-Fe^{III}–OOH, (Eq. (9)). Support to this assumption is found in a similar ESI experiment conducted in the presence of $H_2{}^{18}O_2$ that demonstrates that this specie contains two oxygen atoms derived from labeled hydrogen peroxide.

$$\begin{array}{lll} Fe^{III} + BLM + H_2O_2 & \longrightarrow & [BLM\text{-}Fe^{III}\text{-}OOH]^{2+} \\ {}^{16}O & & m/z\ 751.3 \\ {}^{18}O & & 753.3 \end{array} \quad (9)$$

MS/MS spectra obtained both on unlabeled and labeled species showed that the peroxide O–O bond is labile and may be cleaved

with loss of OH. When activated bleomycin is produced from Fe^{II}BLM and O_2, again the peak centered at *m/z* 751.3 is observed. The peak amplitude is maximal after 10 sec and disappeared after 2 min. Interestingly, when bleomycin is activated with PhIO as oxidant, the production of the expected iron oxene complex O=Fe(V)BLM could not be detected (Sam et al., 1995). Also monomeric Ru(IV)-oxo species were not observed during the oxidation of Ru^{II}BLM either with O_2, H_2O_2, or PhIO (Mouzopoulou et al., 2001). A μ-oxo Ru^{IV}-BLM dimer is likely formed in these conditions as suggested by many spectroscopic evidences, including ESI-MS.

The Fe atom in BLM is believed to be bonded to five nitrogen atoms and a very simple model of its active site may be obtained by complexation of Fe with *N,N,N′-Tris*(2-pyridylmethyl)-ethane-1,2-diamine ligands L_5 (Mialane et al., 1999). Iron complexes of L_5 catalyze the oxidation of alkenes and polyaromatic compounds by H_2O_2. The occurrence of a hydroperoxide form $[L_5\text{-}Fe^{III}\text{–}OOH]^{2+}$ upon reaction with hydrogen peroxide, similar to activated bleomycin, was proposed by Toftlund using EPR spectroscopy (Bernal et al., 1995) and confirmed by ESI-MS.

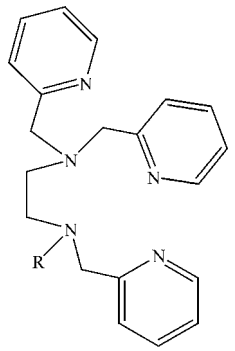

L_5 R=CH_3

The mass spectrum of methanol solutions of $[L_5\text{-}Fe^{II}Cl]Cl$ are characterized by peaks centered at *m/z* 438, corresponding to $[L_5\text{-}Fe^{II}Cl]^+$. Addition of H_2O_2 caused the appearance of a new signal at *m/z* 218, corresponding to the doubly charged entity $[L_5\text{-}Fe^{III}\text{–}OOH]^{2+}$ and typified by a purple color. Upon adding a base, either aqueous NaOH or Et_3N, a blue color appeared, stable for 15 min at room temperature (Simaan et al., 1999). The ESI-MS spectrum of this solution exhibit a peak at *m/z* 435 attributed to $[L_5\text{-}Fe^{III}\text{–}O_2]^+$, also on the bases of the isotope pattern. The structure suggested for this species by Girerd should contain a peroxo group linked in a η^1-or, more likely, in a side-on η^2-mode, (Scheme 2 and Eq. (10)).

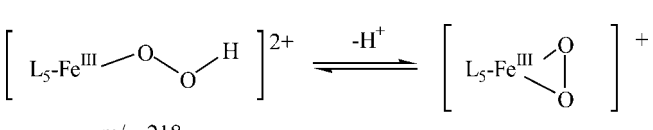

m/z 218 m/z 435

(10)

Similar findings were reported also when L_5 has R=CH_2Py as substituent (Simaan et al., 2000) and by the McKenzie's group using a mononuclear Fe^{II} complex ligated to modified L_5-like ligands, that is, bztpen (Jensen et al., 1999; Hazell et al., 2002). ESI-MS was used to study the formation of the purple Fe^{III}

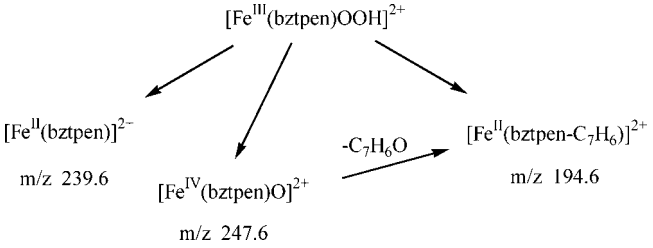

SCHEME 11.

hydroperoxide complex and its base-mediated transformation to the blue Fe^{III} peroxide derivative $[Fe(bztpen)(OO)]^+$. Collision-induced dissociation of the $[Fe(bztpen)OOH]^{2+}$ ionic species produced ions at *m/z* 247.6, 239.6, and 194.6, assigned as depicted in Scheme 11. MS/MS experiments demonstrated as the ions at *m/z* 194.6 may be formed through two independent precursors: (i) the Fe–hydroperoxo complex and (ii) the ferryl species. In the latter case, an intramolecular oxo transfer from the ferryl to the dangling benzyl to generate benzaldeyde, *via* an oxidative cleavage of the bztpen ligand, seems a plausible route.

By contrast, the CID spectrum of the peroxo derivative $[Fe(bztpen)(OO)]^+$ *m/z* 511.2 does not show any peak assignable to the ferryl species Fe^{IV}(bztpen)(O). The interesting conclusion reported by the authors assesses that the facile cleavage of the O–O bond in the hydroperoxide complex compared with the peroxo $[Fe(bztpen)(OO)]^+$ derivative, observed in MS/MS experiments, is in agreement with the higher reactivity showed by the former complex in solution. Based on similar arguments, Fe hydroperoxide species are proposed as precursors of highly oxidizing ferryl intermediates involved in DNA degradation processes catalyzed by bleomycin (Hazell et al., 2002).

The first experimental evidence that an iron (III) hydroperoxide, active in DNA cleavage, may interact with the DNA chain was obtained by the Nishida group using ESI-MS (Kobayashi et al., 2000). The mass spectrometric experiments were based on a comparison of the interaction of a DNA chain with Fe^{III}–bleomycin or the binuclear Fe^{III} complex Fe_2(HPTP)$Cl_4(ClO_4)$. In the latter case, the formation of a signal at *m/z* 1,430.6 was observed, assigned to the species [(12-mer)$[Fe_2(OH)Cl_2(HPTP)]^{2+}$-$5H^+$]$^{3-}$ where the binuclear complex is possibly bound to the DNA chain at the oxygen atoms of the phosphoric group. The addition of H_2O_2 to this solution induced the disappearance of the signal at *m/z* 1,430.6 and the formation of new peaks centered at *m/z* 1,412.2, shifting at *m/z* 1,413.4 when $H_2{}^{18}O_2$ was used, and identified as the DNA-bound hydroperoxo diiron(III) [(12-mer)$[Fe_2(HPTP)(HOO^-)]^{4+}$-$7H^+$]$^{3-}$.

The pentadentate ligand 2,6-*bis*[methoxybis(2-pyridyl)-methyl]pyridine **2** is capable of stabilizing the Fe^{II} center affording complex **3**, catalytically active in the oxidation of alkanols with hydrogen peroxide (de Vries et al., 1997). The reaction of **3** with H_2O_2 was followed by ESI-MS that indicated the initial oxidation of the Fe^{II} ion to Fe^{III}, followed by coordination of the oxidant to form a hydroperoxo species, as depicted in Equation (11). Also in this case, an end-on hydroperoxide structure was proposed, capable to undergo acid–base equilibria to afford $[Fe^{III}\text{–}O_2]^+$ species bound in a side-on η^2-mode, as unequivocally proved by resonance Raman spectroscopy, (Eq. (11)) (Ho et al., 1999). Protonation of the peroxo species is essential for alkane hydroxylation.

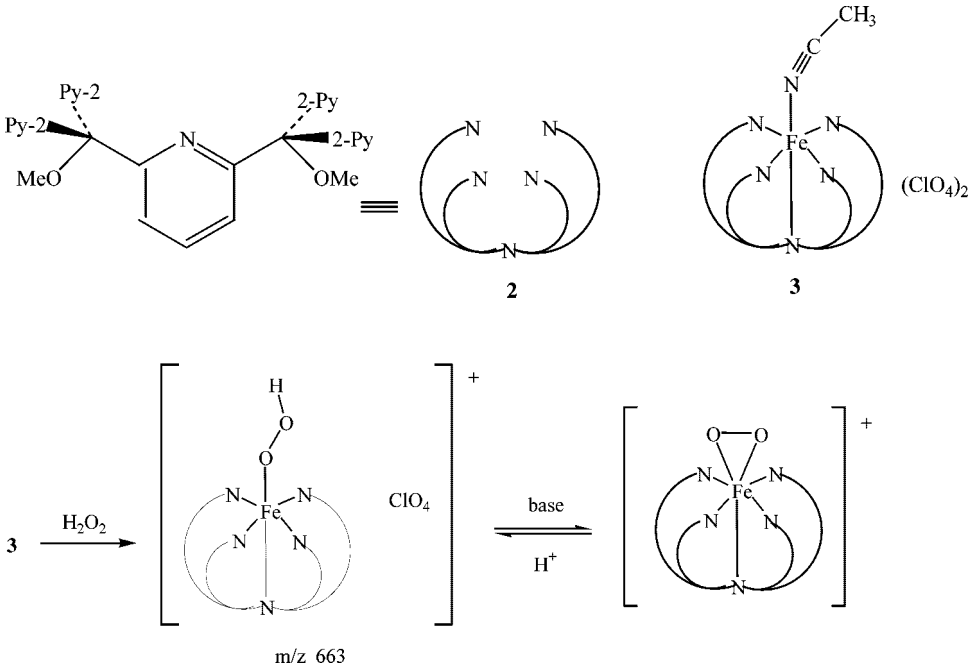

(11)

Formation of end-on Fe^{III}–OOH species containing a phenol group was detected for [Fe(Me-enph)Cl]PF_6 derivatives in the presence of H_2O_2 (Okutsu, Ito, & Nishida, 1999).

Mononuclear non-heme iron complexes have shown to catalyze alkane hydroxylation as well as olefin epoxidation and *cis*-dihydroxylation using H_2O_2 as oxidant (Costas et al., 2004). In general, the catalyst have iron(II) centers coordinated to tetradentate N4 ligands such as TPA **4** and BPMEN **5** that convert to Fe^{III} forms upon treatment with H_2O_2. Based on reaction behavior, these catalysts have a common Fe^{III}–OOH intermediate whose spin state may be categorized into two classes: class A catalyst characterized by low-spin Fe^{III}–OOH intermediates and class B catalysts that afford high-spin Fe^{III}–OOH intermediates (Fujita, Costas, & Que, 2003)

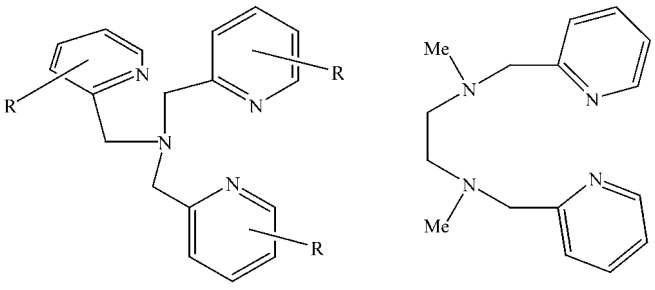

4 **5**

In the oxidations carried out by class A catalysts, the initial Fe^{III}–OOH species is converted to a *cis*-(HO)Fe^{V}=O oxidant in a water-assisted mechanism and the related details are discussed in section IV. Category B catalysts afford *cis*-diol products with both oxygen atoms from H_2O_2, (Eq. (12)).

Activation of the O–O bond is proposed to occur *via* an Fe^{III}-η^2–OOH that may isomerize to an oxidant with nucleophilic preferences (Fujita, Costas, & Que, 2003).

B. Alkylperoxo

Titanium trialkanolamine complexes are very active and selective catalysts for enantioselective sulfoxidation reaction (Bonchio et al., 1997, 1999, 2003a). The catalyst precursor is formed *in situ* by interaction of titanium(IV) isopropoxide and enantiopure trialkanolamine ligands. Such tetradentate ligand binds the metal forming a robust titanatrane core, which maintains its structure also in hydroxylic solvents or in the presence of acid. Depending on the relative concentration of metal and ligand, several polynuclear aggregates may be formed in solution. By subsequent addition of *t*-butyl hydroperoxide, all the pre-catalysts are converted into the mononuclear active species, as indicated in Equation (13). The nature of the active alkyl peroxidic species was elucidated by combination of ESI-MS and conventional low-temperature NMR techniques.

In the absence of TBHP, several species have been identified on the basis of MS/MS analysis and comparison between the theoretical and experimental cluster ion peaks. The overall spectrum shows the presence of several species that can be originated in equilibria involving mononuclear and polynuclear titanium cores (up to three titanium centers) and all the

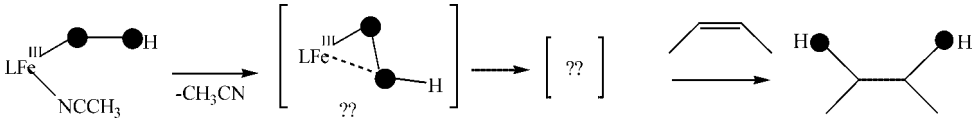

(12)

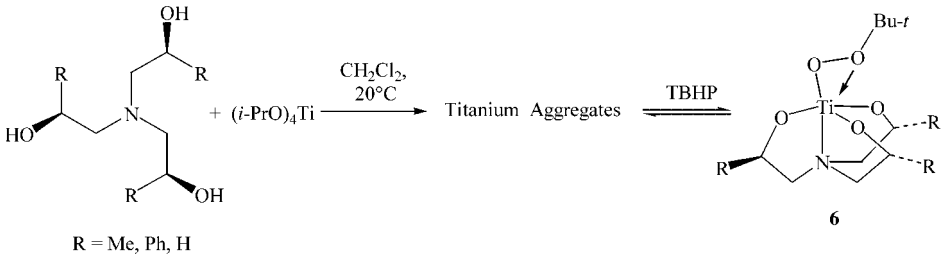

(13)

oxygen-containing nucleophiles present in solution, water methanol, and trialkanolamine (Bonchio et al., 1997). Some of these species were also present in the positive-ion ESI mass spectrum, recorded when TBHP is added in acidic $CHCl_3$ solution, situation which corresponds to catalytic enantioselective sulfoxidation reaction. Furthermore, when excesses of TBHP are added, the protonated peroxy complex **6** is completely identified and characterized ($m/z = 326$ for R=CH_3), (see Scheme 12) (Bonchio et al., 1999). In particular, the cluster ion peak distribution and the related MS/MS analysis are reliable with the monomeric nature of the alkylperoxo species. The fragmentation pattern observed is consistent with the breaking of the O–Bu^t bond (M^+-C_4H_8) and of the peroxidic O–O bond (M^+-C_4H_8O). This latter decomposition is also consistent with the O–O bond scission proposed as key step in the sulfoxidation reaction.

Interestingly, subsequent ESI-MS studies have been used to obtain evidence concerning the coordination of sulfoxides to the active titanium monomeric alkylperoxidic species **6** (Bonchio et al., 2003a). In the following Equation (14) are collected the main figures obtained with CID experiments, which elucidated the "strong" coordination of the sulfoxide moiety to the titanium core.)

ESI-MS has been used in the characterization of a transient blue species that has been shown to oxidize alcohols and is proposed to be involved in the oxidation of alkanes in $[Fe^{III}_2O(TPA)_2]^{4+}$/$Bu^tOOH$ systems. The reaction of $[Fe_2O(TPA)_2(H_2O)(ClO_4)](ClO_4)_3$ with an excess of benzyl alcohol affords a mononuclear complex **7** formulated as $[Fe(TPA)(OCH_2Ph)(ROH)](ClO_4)_2$ (R=H, CH_2Ph). Addition of Bu^tOOH to **7** produced a blue intermediated **8** that has been identified with the help of ESI-MS (Kim et al., 1996). The mass values of m/z 542, 534, and 452, respectively and isotope distribution patterns formulate **8** as an equilibrium mixture of two species $[Fe(TPA)(OOBu^t)(ROH)](ClO_4)_2$ (R=H, CH_2Ph), with the observed ions derived from the parent ion $[Fe(TPA)(OOBu^t)(ROH)](ClO_4)^+$, according to Scheme 13. The MS/MS spectra of the three ions showed loss of the Bu^tOO fragment and, only for the ion at m/z 452, release of the Bu^tO moiety corresponding to the homolysis of the FeO–OBu^t bond, to form $[Fe^{IV}(O)(TPA)(OH)]^+$ ionic species.

Mononuclear $[Fe^{IV}(O)(TPA)(CH_3CN)]^{2+}$ can be obtained by reaction of its iron (II) precursor with Bu^tOOH in CH_3CN and from $[Fe^{II}(BPMCN)(OTf)_2]$/Bu^tOOH in non-coordinating CH_2Cl_2 (BPMCN = *N,N′-bis*(2-pyridylmethyl)-*N,N′*-dimethyl-trans-1,2-diaminocyclohexane) (Jensen et al., 2005). In the latter case, clear evidence was provided, including ESI-MS, to support the Fe^{IV}-oxo derivative $[Fe^{IV}(O)(BPMCN)(OTf)]^+$ m/z 545 as derived from the alkylhydroperoxo complex $[Fe^{IV}$ (BPMCN)(O-H)$(OOBu^t)(OTf)_2]$, (Scheme 14).

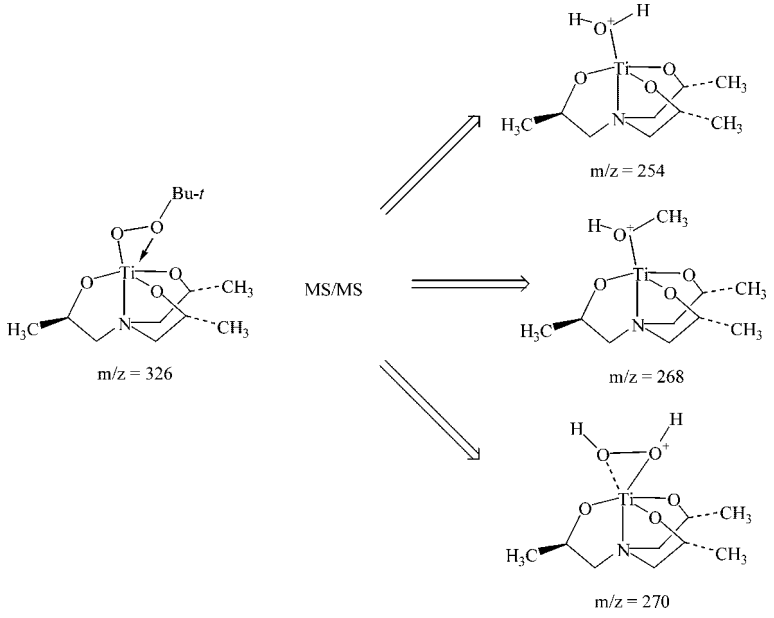

SCHEME 12.

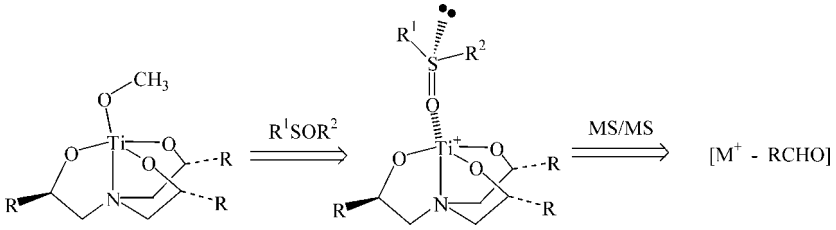

(14)

IV. METAL-OXO

Metal-salen complexes **9** (metal = Mn, Cr), introduced by Kochi et al. (1983) as simplified synthetic models of porphyrin analogs and modified by Jacobsen (Zhang et al., 1990) and Katsuki (Irie et al., 1990) through the introduction of a chiral salen catalyst, represented an efficient breakthrough in the epoxidation of non-functionalized alkenes with different oxidants at high enantioselectivity.

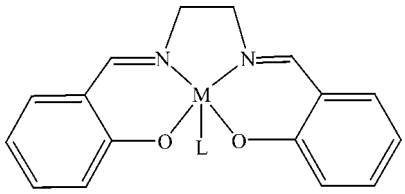

9

A variety of alkenes have, thus, been epoxidized with simple oxygen donors such as PhIO, NaClO, H_2O_2, Oxone, and an optimal enantioselectivity for a given substrate could be achieved by choosing the proper catalyst and reaction conditions, (Eq. (15)) (McGarrigle & Gilheany, 2005).

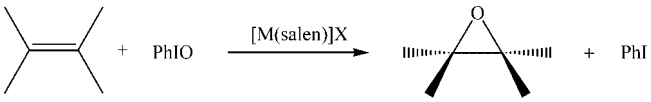

(15)

It is generally accepted that Mn- and Cr-salen complexes catalyze the oxidation of organic substrates through formation of a high-valent metal-oxo species (salen)M=O. The salient mechanistic aspects of this epoxidation have been investigated by many authors. In particular and with the help of mass spectrometric techniques, Plattner addressed his studies on two basic points of the mechanism: (i) how is the oxygen transferred to the metal center achieved and (ii) what are the species produced upon oxidation (Plattner, 2003). By submitting to electrospray *in situ* mixtures of $[Mn^{III}(salen)]^+$ and suitable oxygen transferring agent, that is, iodosobenzene (PhIO), formation of oxidized species were observed, corresponding to the oxo complex $[(salen)Mn^{V}{=}O]^+$ (*m/z* 337) and the μ-oxo-bridged doubly charged dimer with two terminal PhIO ligands $[PhIO(salen)Mn\text{-}O\text{-}Mn(salen)OIPh]^{2+}$ (*m/z* 549) (Feichtinger & Plattner, 1997; Feichtinger & Plattner, 2000). The collision-induced fragmentation of this latter dimeric ion gives rise to the decomposition product derivatives of Mn^{III}- and Mn^{V}-oxo, (Eq. (16)). These findings represented the first experimental evidence for the formation (conproportionation) and decomposition (disproportionation) of a μ-oxo bridged Mn^{IV} dimer acting as reservoir of the catalytically active species involved in the oxidation reaction (Feichtinger & Plattner, 2001).

$$[PhIO(salen)Mn-O-Mn(salen)OIPh]^{2+} \rightarrow [PhIO(salen)Mn^{III}]^+ + [PhIO(salen)Mn^{V}=O]^+ \quad (16)$$

Interestingly, when $[PhIO(salen)Mn^{III}]^+$ species is mass selected and submitted to MS/MS experiments, formation of $[(salen)Mn^{V}=O]^+$ is observed because of the easy fragmentation of the O–I bond of the coordinated iodosobenzene, (Eq. (17)). CID experiments on the oxo complex $[PhIO(salen)Mn^{V}=O]^+$ mainly leads to the loss of iodosobenzene, (Eq. (18)).

$$\underset{m/z\,541}{[PhIO(salen)Mn^{III}]^+} \rightarrow \underset{m/z\,337}{[(salen)Mn^{V}=O]^+} \quad (17)$$

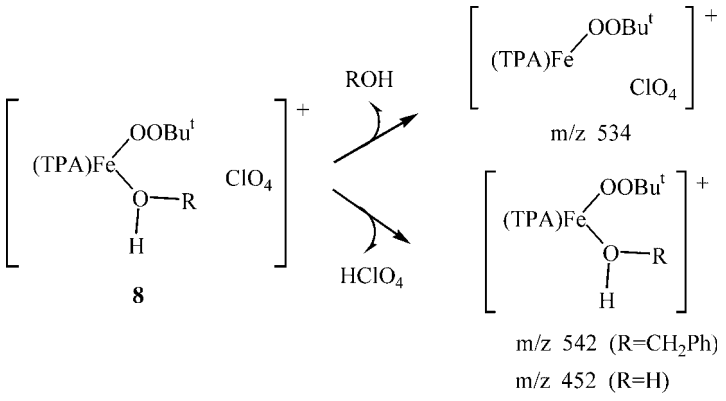

8

SCHEME 13.

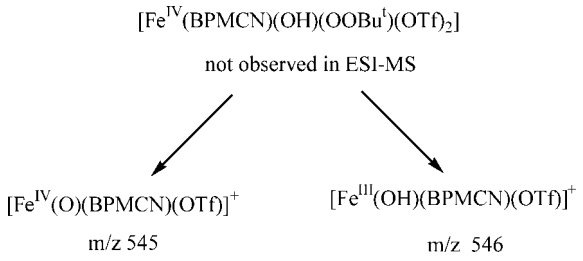

SCHEME 14.

$$[\underset{m/z\,557}{\mathrm{PhIO(salen)Mn^{V}=O}}]^{+} \rightarrow [\underset{m/z\,337}{\mathrm{(salen)Mn^{V}=O}}]^{+} \quad (18)$$

The capability of oxo manganese (V) species to transfer oxygen to suitable organic substrates in the gas phase was equally demonstrated by collision experiments. When $[(salen)Mn^{V}{=}O]^{+}$ ions are mass selected and submitted to CID experiments with either Ar or Xe collision gases, no fragmentation can be obtained, (Eq. (19)). However, if the inert gas is replaced with oxygen acceptors like sulfides or electron-rich olefins, formation of $[(salen)Mn^{III}]^{+}$ ions, that is, the reduction product of the oxidation reaction, is detected, (Eq. (20)), thus indirectly demonstrating that oxygen transfer to a substrate is taking place.

$$[(salen)Mn^{V}=O]^{+} \xrightarrow{\text{Ar or Xe}} [(salen)Mn^{V}=O]^{+} \quad (19)$$

$$[(salen)Mn^{V}=O]^{+} \xrightarrow{\text{Sulfide or olefin}} [(salen)Mn^{III}]^{+} \quad (20)$$

The effects of various substituents in the 5- and 5′-positions of the salen as well as those pertained to the axial ligands have been evaluated in detail. Electron-withdrawing substituents on salen and additional axial ligands decrease the stability thus enhancing the reactivity of the Mn=O moiety (Plattner et al., 2000; Feichtinger & Plattner, 2001). The role of axial ligation on geometry and reactivity of the high-valent oxo complex appeared quite drastic.

Manganese complexes derived from TMTACN ligands **10** have been found to be highly active catalysts both for low-temperature bleaching and for the epoxidation of alkenes with hydrogen peroxide. These derivatives are particularly active also in the oxidation of azonaphthol dyes and phenols (Gilbert et al., 2004).

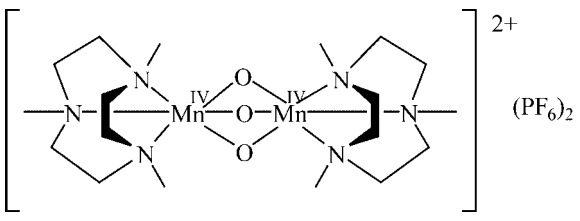

10

The oxidation of phenolic derivatives with H_2O_2 catalyzed by $[Mn_2^{IV}(\mu\text{-}O)_3(TMTACN)_2](PF_6)_2$ **10** has been investigated by the use of ESI-MS (Gilbert et al., 1998; Gilbert et al., 2004). When H_2O_2 is added to a mixture of **10** and *para*-methoxy phenol, as model substrate, two peaks dominate the mass spectrum at *m/z* values of 470 and 486, respectively, identified as $[TMTACN\text{-}Mn^{III}(5,5'\text{-dimethoxy-}2,2'\text{-bisphenolate})]^{+}$ **11** and the related Mn^{V}-oxo derivative **12**.

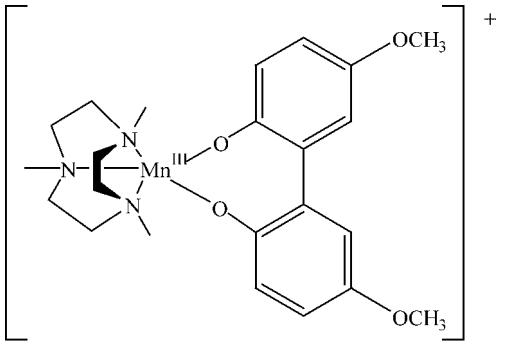

11

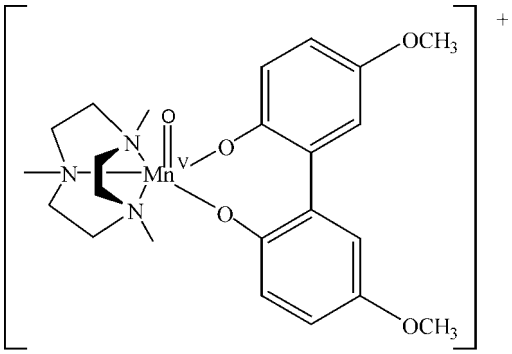

12

When the reaction is carried out in the presence of $H_2{}^{18}O_2$, the signal pertaining to **12** shifted at *m/z* 488, whereas if $H_2{}^{18}O$ is used, no incorporation was observed. These experiments identified hydrogen peroxide as the source of the oxo-oxygen. On the basis of ESI-MS and EPR data, a catalytic cycle for the oxidation of phenols has been proposed in which the key intermediates were unequivocally characterized by the former technique, (Scheme 15).

In the oxidation of azonaphthol dyes with H_2O_2, ESI-MS investigations provide evidence for the formation and reaction of $TMTACN\text{-}Mn^{IV}(OH)_3$ key intermediates (Gilbert et al., 2003).

The addition of carboxylic acids, that is, CCl_3COOH, in the $[Mn_2^{IV}(\mu\text{-}O)_3(TMTACN)_2]^{2+}/H_2O_2$ oxidation system enables the tuning of the catalyst's selectivity toward *cis*-dihydroxylation and epoxidation (de Boer et al., 2005). In this case, ESI-MS put in evidence **13** as the immediate precursor of the active species.

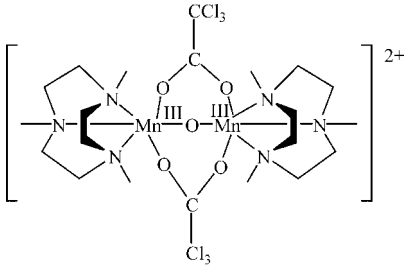

13

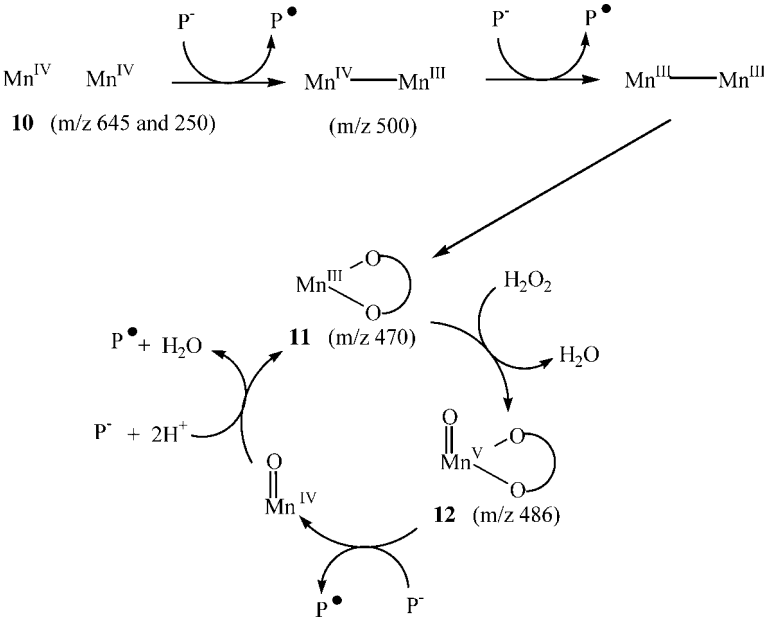

SCHEME 15. P = phenol; P˙ = phenol radical

As discussed in Section III, Que and co-workers have shown as Fe^{III}–OOH species coordinated to tetradentate N4 ligands such as TPA **4** and BPMEN **5**, key intermediates in *cis*-dihydroxylation and epoxidation processes with H_2O_2, give rise to two categories of catalysts that is class A and B. For category A, the initial Fe^{III}–OOH intermediate is converted to a *cis*-$(HO)Fe^{V}$=O oxidant in a water-assisted mechanism. Determinant support to this proposal is the evidence that both the epoxide and the diol products incorporate ^{18}O from $H_2{}^{18}O$, (Eq. (21)) (Quiñonero et al., 2005).

ESI-MS experiments have been proved to be an excellent tool for establishing the molecular composition of the transient species (Kim et al., 1997; Chen et al., 2002). When the precursor $[Fe^{II}(TPA)(CH_3CN)_2](ClO_4)_2$ and H_2O_2 are introduced into the mass spectrometer, *via* a mixing tee, two signals are observed at *m/z* 462 and 478 corresponding to $[Fe^{III}(TPA)(OH)(ClO_4)]^+$ and $[Fe^{III}(TPA)(OOH)(ClO_4)]^+$, respectively. The hydroperoxo derivative is not affected by the presence of $H_2{}^{18}O$ and fragments with formation of ionic species at *m/z* 445 and 461 in MS/MS experiments, (Scheme 16).

When the ESI-MS spectra are recorded in the presence of styrene, new signals are observed at *m/z* 482, 500, 516, and 582 in addition to the already described *m/z* 462 and 478 ionic species. The most intense peak corresponds to a combination of the Fe^{III}–OOH intermediate and styrene (*m/z* 478 + 104 = 582) that in principle may be formulated in different ways. The lack of expulsion of styrene, in the corresponding daughter ion mass spectrum, supports a tight combination of the alkene and the peroxide, or more likely the *cis*-$(HO)Fe^{V}$=O moiety, as in **14**.

With similar arguments, the structures of the remaining ions are proposed as shown in Equation (22) and in structures **15** and **16**. Thus, the product diol coordinates to the metal center in the course of a turnover and is presumably displaced by H_2O_2 to initiate the next round of catalysis.

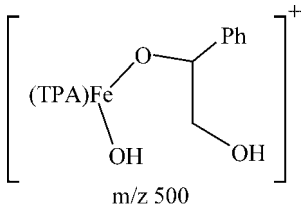

m/z 500

15

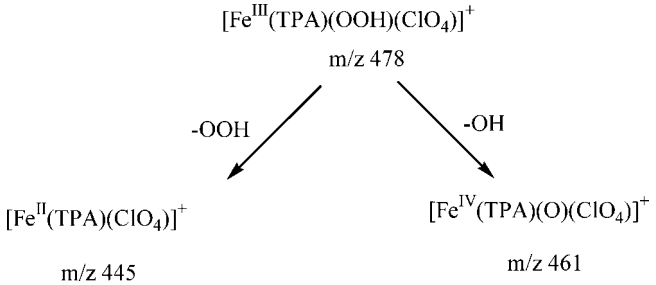

SCHEME 16.

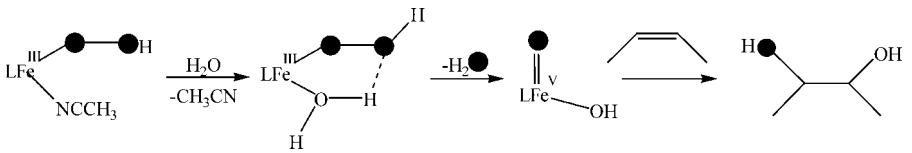

(21)

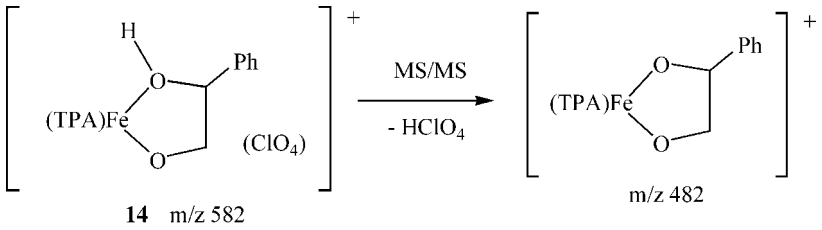

14 m/z 582 m/z 482 (22)

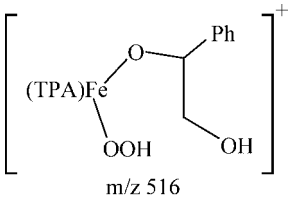

m/z 516

16

High-valent iron-oxo intermediates are frequently invoked in the catalytic cycles of mononuclear enzymes that activate O_2 for important biological oxidations. Que and co-workers have characterized a family of synthetic complexes that form Fe^{IV}=O intermediates able to activate even the strong C–H bond in cyclohexane (Rohde et al., 2003). The oxo-iron units are stabilized by tetraaza ligands N4 as tetramethylcyclam TMC **17**, or pentaaza ligands as N4Py **18** and BnTPEN **19**.

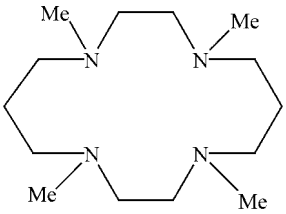

TMC **17**

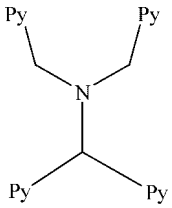

N4Py **18**

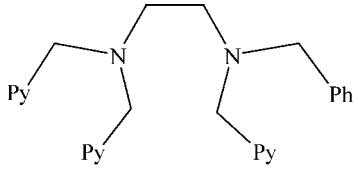

BnTPEN **19**

ESI-MS provides strong evidence to the formation of Fe^{IV}=O intermediates. When the precursor $[Fe^{II}(TMC)(OTf)_2]$ is treated with PhIO in CH_3CN at −40°C, formation of a green intermediate is observed, characterized by prominent ions at *m/z* 184.4 and 476.9. The mass and isotopic distribution patterns correspond to $[Fe^{IV}(O)(TMC)(NCCH_3)]^{2+}$ for the former and $[Fe^{IV}(O)(TMC)(OTf)]^{+}$ for the latter species. These features upshift of 2 Da. when $PhI^{18}O$ is used and disappear from the mass spectrum upon reaction with Ph_3P (Rohde et al., 2003). Similarly, when $[Fe^{II}(N4Py)(CH_3CN)](ClO_4)_2$ or $[Fe^{II}(BnTPEN)(OTf)](OTf)$ are reacted with excess of solid PhIO in CH_3CN formation of $[Fe^{IV}(O)(N4Py)(ClO_4)]^{+}$ *m/z* 538.0559 and $[Fe^{IV}(O)(BnTPEN)(OTf)]^{+}$ *m/z* 644.1227 was detected by high-resolution ESI-MS (Kaizer et al., 2004).

Availability of ESI-MS has been critical for the recent successful characterization of *bis*(μ-oxo)dimetal cores $[M_2(\mu\text{-}O_2)]^{n+}$ of Fe, Co, Ni, Cu (Que & Tolman, 2002). Of particular interest is the case of (μ-oxo)diiron species, model intermediates in methane monoxygenase (MMO) processes. A number of $[Fe_2^{III}(O)_2(L)_2](ClO_4)_2$, where L are ring-alkylated derivatives 6-Me-TPA, 6-Me_3-TPA (TPA = **4**), have been synthesized and submitted to one-electron oxidation. The resulting species is proposed to have an Fe^{III}–O–Fe^{IV}=O structure, derived from the isomerization of the $Fe_2(\mu\text{-}O)_2$ diamond core as shown in Equation (23), thus demonstrating the accessibility of a terminal Fe^{IV}=O unit in a non-heme environment. ESI-MS was used to characterize this latter complex and peaks corresponding to $[Fe_2(O)_2(6\text{-}Me_3\text{-}TPA)_2](NO_3)(ClO_4)^{+}$ *m/z* 969 and $[Fe_2(O)_2(6\text{-}Me_3\text{-}TPA)_2](ClO_4)_2^{+}$ *m/z* 1,006 have been observed (Zheng et al., 2000). Clusters of positive ions corresponding to the above ionic species plus a water molecule, *m/z* 987 and 1,024 are equally present in the mass spectra, suggesting that the cation having the Fe^{III}–O–Fe^{IV}=O structure is best formulated as $[Fe_2(O)_2(H_2O)(L)_2]^{3+}$, (Eq. (23)).

Several metal-oxo complexes, including MnO_4^-, $Cr_2O_7^{2-}$, CrO_3Cl^-, RuO_4^-, $RuO_2Cl_3^-$ and $[Ru(TMC)O_2]^{2+}$ used as stoichiometric or catalytic oxidants and involved in several enzymatic oxidations, have been characterized by ESI-MS (Lau et al., 1994). The oxidative capability of the latter complex was demonstrated by studying its reaction with potassium iodide. The base peak at *m/z* 195 characterizing the precursor was shifted at *m/z* 196, consistent with the reduction of $[Ru^{IV}(TMC)O_2]^{2+}$ to $[Ru^{IV}(TMC)O(H_2O)]^{2+}$, whose formation was confirmed also by UV-vis.

cis-Dioxoruthenium complexes $[Cn(CF_3CO_2)Ru^{IV}O_2]ClO_4$ **20** oxidize di-substituted alkynes to 1,2-diketones in good yields, (Eq. (24), Cn=TMTACN). It has long been postulated that this oxidations proceed *via* a putative cyclic intermediate formally generated by a [3 + 2] cycloaddition; however, the existence of the cycloadduct was not clearly proved.

ESI-MS was used to prove the occurrence of the postulated cyclic intermediates, observed during the stoichiometric oxida-

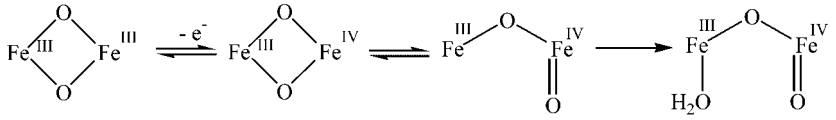

(23)

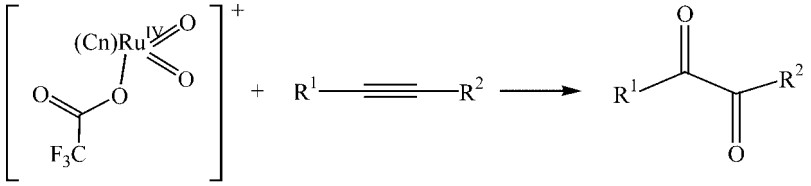

(24)

20

tion of alkynes with dioxoruthenium complexes (Che et al., 2000). When **20** is mixed with an excess of *bis*(trimethylsilyl)acetylene (R^1=R^2=Si(Me)$_3$) in CH_3CN and submitted to MS analysis, a single prominent ion cluster is formed at *m/z* 588, unequivocally assigned to the cyclic intermediate **21**. Similarly, other alkynes afforded cyclic intermediates of structure **21**-like, together with the presence of mass peak clusters assigned to $[Cn(CF_3CO_2)Ru^{II}(CH_3CN)_2]^+$ ions.

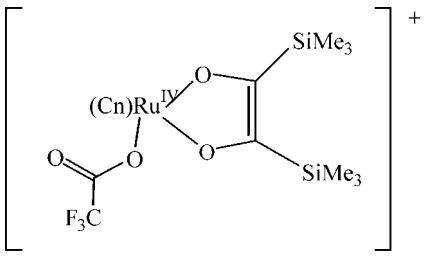

21 (m/z 588)

V. CONCLUSIONS

In this overview, we have collected and discussed some of the most important applications of mass spectrometry, in particular of ESI-MS, to the detection and characterization of reaction intermediates. The existence of several high-valent metal oxo-, -peroxo, and -peroxy derivatives, key intermediates in the oxyfunctionalization of organic substrates, can be probed with this technique, particularly when the more traditional methods are inappropriate. The combined use of ESI-MS in association with other spectroscopic techniques and theoretical calculations demonstrated to be a powerful tool for the detailed understanding of the species involved in solution and their reaction mechanisms. A vast field of possible applications remains unexplored including the analysis of polyoxometalates, a very important class of catalyst that are recently achieving a great deal of attention in oxidation chemistry (Bonchio et al., 2003b; Howarth, Pettersson, & Andersson, 2001). For this class of aggregate species, the ESI-MS analysis can be in some cases even simpler than the NMR one, as it has been indicated for hexatungstate peroxo derivative (Howarth, Pettersson, & Andersson, 2001). In the case of highly charged mono-lacunary Keggin-type polyoxotungstates α-$[XW_{11}O_{39}]^{p-}$ (X = Si, P; p = 8, 7), ESI-MS analysis provided a straightforward tool for the solution characterization. Double and triple charged quasi-molecular ion peaks were observe and identified on the basis of theoretical simulation of the isotopic cluster distributions and fragmentation modes observed with MS/MS technique (Bonchio et al., 2003b).

ABBREVIATIONS AND ACRONYMS

Bipy	*bis*(2,2′-bipyridine)
BLM	bleomycin
BnTPEN	*N*-benzyl-*N*,*N*′,*N*′-*tris*(2-pyridylmethyl)-1,2-diaminoethane
BPMCN	*N*,*N*′-*bis*(2-pyridylmethyl)-*N*,*N*′-dimethyl-*trans*-1,2-diaminocyclohexane
BPMEN	*N*-*N*′-dimethyl-*N*-*N*′-*bis*(2-pyridylmethyl)-1,2-diaminoethane
bztpen	*N*-benzyl-*N*,*N*′,*N*′-*tris*(2-pyridylmethyl)-ethane-1,2-diamine
CID	collision-induced dissociation
EPR	electron paramagnetic resonance
ESI-MS	electrospray ionization mass spectrometry
HPTP	*N*,*N*,*N*′,*N*′-tetrakis(2-pyridylmethyl)-1,3-diamini-2-propanol
IR	infrared
MALDI- TOF	matrix-assisted laser desorption-ionization-time-of-flight
Me_3-tpa	*tris*(6-methyl-2-pyridylmethyl)amine
MS/MS	tandem mass spectra
NMR	nuclear magnetic resonance
N4Py	*N*,*N*-*bis*(2-pyridylmethyl)-*N*-*bis*(2pyridyl)-methylamine
OTf	trifluoromethanesulfonate
salen	*N*,*N*′-*bis*(salicylidene)ethyl-enediamine
TBHP	*ter*-butyl hydroperoxide
TMC	1,4,8,11-tetramethyl-1,4,8,11-tetraazacyclotetradecane
TMTACN	1,4,7-trimethyl-1,4,7-triazacyclononane
TPA	tris(2-pyridylmethyl)amine
UV-vis	ultraviolet visible

REFERENCES

Adam W, Malisch W, Roschmann KJ, Saha-Möller CR, Schenk WA. 2002. Catalytic oxidations by peroxy, peroxo and oxo metal complexes: An interdisciplinary account with a personal view. J Organomet Chem 661:3–16.

Aleksandrov ML, Gall LN, Krasnov VN, Nikolaev VI, Pavlenko VA, Shkurov VA. 1984. Extraction of ions from solutions under atmospheric pressure: A method of mass spectrometric analysis of bioorganic compounds. Doklady Akademii Nauk 277:379–383.

Andersson I, Angus-Dunne S, Howarth O, Pettersson L. 2000. Speciation in vanadium bioinorganic systems 6. Speciation study of aqueous peroxovanadates, including complexes with imidazole. J Inorg Biochem 80:51–58.

Bernal I, Jensen IM, Jensen KB, McKenzie CJ, Toftlund H, Tuchagues J-P. 1995. Iron(II) complexes of polydentate aminopyridyl ligands and an exchangeable sixth ligand; reactions with peroxides. Crystal structure of $[FeL^1(H_2O)][PF_6]_2.H_2O$ [L^1 = *N,N-bis*-(6-methyl-2-pyridylmethyl)-*N,N′-bis*(2-pyridylmethyl)ethane-1,2-diamine]. J Chem Soc Dalton Trans 22:3667–3675.

Bonchio M, Licini G, Modena G, Moro S, Bortolini O, Traldi P, Nugent WA. 1997. Use of electrospray ionization mass spectrometry to characterize chiral reactive intermediates in a titanium alkoxide mediated sulfoxidation reaction. Chem Commun 869–870.

Bonchio M, Licini G, Modena G, Bortolini O, Moro S, Nugent WA. 1999. Enantioselective Ti(IV) sulfoxidation catalysts bearing C_3-symmetric trialkanolamine ligands: Solution speciation by ^{1}H-NMR and ESI-MS analysis. J Am Chem Soc 121:6258–6268.

Bonchio M, Bortolini O, Carraro M, Conte V, Primon S. 2000. Vanadium catalyzed reduction of dioxygen to hydrogen peroxide: An oscillatine process. J Inorg Biochem 80:191–194.

Bonchio M, Bortolini O, Conte V, Moro S. 2001a. Characterization and reactivity of triperoxo vanadium complexes in protic solvents. Eur J Inorg Chem 2913–2919.

Bonchio M, Bortolini O, Conte V, Primon S, 2001b. Aerobic oxidation of isopropanol catalysed by peroxovanadium complexes: Mechanistic insights. J Chem Soc Perkin Trans 2:763–765.

Bonchio M, Bortolini O, Licini G, Moro S, Nugent WA. 2003a. On the mechanism of the oxygen transfer to sulfoxides by (peroxo)[tris(hydroxyalkyl)amine]Ti^{IV} complexes. Evidence for a metal-template-assisted process. Eur J Org Chem 507–511.

Bonchio M, Bortolini O, Conte V, Sartorel A. 2003b. Electrospray Behavior of Lacunary Keggin-type Polyoxotungstates $[XW_{11}O_{39}]^{p(}$, (X= Si, P). Mass Spectrometric Evidence for a Concentration Dependent Incorporation of a MO^{n+} (M= W(VI), Mo(VI), V(V)) unit into the Polyoxometalate Vacancy. Eur J Inorg Chem 699–704.

Bortolini O, Conte V. 2005. Vanadium(V) peroxocomplexes: Structure, chemistry and biological implications. J Inorg Biochem 99:1549–1557.

Bortolini O, Conte V, Di Furia F, Moro S. 1998. Direct evidence of solvent-peroxovanadium clusters by electrospray ionisation mass spectrometry. Eur J Inorg Chem 1193–1197.

Bortolini O, Carraro M, Conte V, Moro S. 1999. Histidine-containing bis-peroxovanadium(V) compounds: Insight into the solution structure by an ESI-MS and ^{51}V-NMR comparative study. Eur J Inorg Chem 1489–1495.

Bortolini O, Carraro M, Conte V, Moro S. 2003. Vanadium-bromoperoxidase-mimicking systems: Direct evidence of a hypobromite-like vanadium intermediate. Eur J Inorg Chem 42–46.

Busch KL, Glish GL, McLuckey SA. 1988. Mass spectrometry/mass spectrometry: Techniques and applications of tandem mass spectrometry. New York: VCH Publishers.

Butler A, Claugue M, Meister GE. 1994. Vanadium peroxide complexes. Chem Rev 94:625–638.

Čsny M, Rehder D, Schmidt H, Vilter H, Conte V. 2000. A ^{17}O-NMR study of peroxide binding to the active center of bromoperoxidase from *Ascophyllum Nodosum*. J Inorg Biochem 80:157–160.

Che C-M, Yu W-Y, Chan P-M, Cheng W-C, Peng S-M, Lau K-C, Li W-K. 2000. Alkyne oxidations by *cis*-dioxoruthenium(VI) complexes. A formal [3 + 2] cycloaddition reaction of alkynes with *cis*-$[Cn^*(CF_3CO_2)Ru^{IV}O_2]ClO_4$ (Cn= 1,4,7-trimethyl-1,4,7-triazacyclononane). J Am Chem Soc 122:11380–11392.

Chen K, Costas M, Kim J, Tipton AK, Que L, Jr. 2002. Olefin *cis*-dihydroxylation versus epoxidation by non-heme iron catalysts: Two faces of an Fe^{III}-OOH coin. J Am Chem Soc 124:3026–3035.

Cole RB, editor. 1997. Electrospray ionization mass spectrometry. Fundamentals, instrumentation and applications. New York: John Wiley & Sons.

Colton R, D'Agostino A, Traeger JC. 1995. Electrospray mass spectrometry applied to inorganic and organometallic chemistry. Mass Spectrom Rev 14:79–106.

Conte V, Bortolini O. 2006. Transition metal peroxides: Synthesis and role in oxidation reactions. In: Rappoport Z, editor. The chemistry of peroxides. Hoboken, NJ: Wiley.

Conte V, Bortolini O, Carraro M, Moro S. 2000. Model for the active site of vanadium-dependent haloperoxidases: Insight into the solution structure of peroxo vanadium compounds. J Inorg Biochem 80:41–49.

Costas M, Mehn MP, Jensen MP, Que L, Jr. 2004. Dioxygen activation at mononuclear iron active sites: Enzymes, models and intermediates. Chem Rev 104:939–986.

Crans DC, Smee JJ, Gaidamauskas E, Yang L. 2004. The chemistry and biochemistry of vanadium and the biological activities exerted by vanadium compounds. Chem Rev 104:849.

de Boer JW, Brinksma J, Browne WR, Meetsma A, Alsters PL, Hage R, Feringa BL. 2005. *cis*-Dihydroxylation and epoxidation of alkenes by $[Mn_2O(RCO_2)_2(tmtacn)_2]$: Tailoring the selectivity of a high H_2O_2-efficient catalyst. J Am Chem Soc 127:7990–7991.

de Vries ME, La Crois RM, Roelfes G, Kooijman H, Spek AL, Hage R, Feringa BL. 1997. A novel pentadentate ligand 2,6-*bis*[methoxybis(2-pyridyl)methyl]pyridine L for mononuclear iron(II) and manganese(II)compounds; syntheis and crystal structures of [FeL(MeCN)][ClO_4]$_2$ and [MnL(H_2O)][ClO_4]$_2$. Chem Commun 1549–1550.

Feichtinger D, Plattner DA. 1997. Direct proof for O=Mn^V(salen) complexes. Angew Chem Int Ed Engl 36:1718–1719.

Feichtinger D, Plattner DA. 2000. Oxygen transfer to manganese-salen complexes: An electrospray tandem mass spectrometric study. J Chem Soc Perkin Trans 2:1023–1028.

Feichtinger D, Plattner DA. 2001. Probing the reactivity of oxomanganese-salen complexes: An electrospray tandem mass spectrometric study of highly reactive intermediates. Chem Eur J 7:591–599.

Fenn JB, Mann M, Meng CK, Wong SF, Whitehouse CM. 1990. Electrospray ionization—Principles and practice. Mass Spectrom Rev 9:37–70.

Fujita M, Costas M, Que L, Jr. 2003. Iron-catalyzed olefin *cis*-dihydroxylation by H_2O_2: Electrophilic versus nucleophilic mechanisms. J Am Chem Soc 125:9912–9913.

Ghiladi RA, Huang H, Moenne-Laccoz P, Stasser J, Blackburn NJ, Woods AS, Cotter RJ, Incarvito CD, Rheingold AL, Karlin KD. 2005. Heme-copper/dioxygen adduct formation relevant to cytochrome *c* oxidase: Spectroscopic characterization of [(^{6}L)Fe^{III}-(O_2^{2-})-Cu^{II}]$^+$. J Biol Inorg Chem 10:63–77.

Gilbert BC, Kamp NWJ, Lindsay Smith JR, Oakes J. 1998. Electrospray mass spectrometry evidence for an oxo-manganese(V) species generated during the reaction of manganese triazacyclononane complexes with H_2O_2 and 4-methoxyphenol in aqueous solution. J Chem Soc Perkin 2:1841–1843.

Gilbert BC, Lindsay Smith JR, Newton MS, Oakes J, Pons i Prats R. 2003. Azo dye oxidation with hydrogen peroxide catalysed by manganese 1,4,7-trimethyl-1,4,7-triazacyclononane complexes in aqueous solution. Org Biomol Chem 1:1568–1577.

Gilbert BC, Lindsay Smith JR, Mairata I Payeras A, Oakes J. 2004. Formation and reaction of O=Mn^V species in the oxidation of phenolic substrates with H_2O_2 catalysed by the dinuclear manganese(IV) 1,4,7-trimethyl-

1,4,7-triazacyclononane complex $[Mn_2^{IV}(\mu\text{-}O)_3(TMTACN)_2]$ $(PF_6)_2$. Org Biomol Chem 2:1176–1180.

Hazell A, McKenzie CJ, Nielsen LP, Schindler S, Weitzer M. 2002. Mononuclear non-heme iron(III) peroxide complexes: Synthesis, characterization, mass spectrometric and kinetic studies. J Chem Soc Dalton Trans 310–317.

Henderson W, Nicholson BK, McCaffrey LJ. 1998. Applications of electrospray mass spectrometry in organometallic chemistry. Polyhedron 17:4291–4313.

Henderson W, Evans C. 1999. Electrospray mass spectrometric analysis of transition-metal halide complexes. Inorg Chim Acta 294:183–192.

Ho RYN, Roelfes G, Hermant R, Hage R, Feringa BL, Que L, Jr. 1999. Resonance raman evidence for the interconversion between an $[Fe^{III}\text{-}\eta^1\text{-}OOH]^{2+}$ and $[Fe^{III}\text{-}\eta^2\text{-}O_2]^{+}$ species and mechanistic implications thereof. Chem Commun 2161–2162.

Howarth OW, Pettersson L, Andersson I. 2001. Aqueous peroxoisopolyoxometalates. In Pope MT, Müller A, editors. Polyoxometalates chemistry. Kluver Academic Publishers 145–159.

Irie R, Noda K, Ito Y, Matsumoto N, Katsuki T. 1990. Catalytic asymmetric epoxidation of unfunctionalized olefins. Tetrahedron Lett 31:7345–7348.

Jensen KB, McKenzie CJ, Nielsen LP, Pedersen JZ, Svendsen HM. 1999. Deprotonation of low-spin mononuclear iron(III)-hydroperoxide complexes give transient blue species assigned to high-spin iron(III)-peroxide complexes. Chem Commun 1313–1314.

Jensen MP, Costas M, Ho RYN, Kaizer J, Mairata I Payeras A, Munch E, Que L, Jr., Rohde J-U, Stubna A. 2005. High-valent nonheme iron. Two distinct iron(IV) species derived from a common iron(II) precursor. J Am Chem Soc 127:10512–10525.

Kaizer J, Klinker EJ, Oh NY, Rohde J-U, Song WJ, Stubna A, Kim J, Munck E, Nam W, Que L, Jr. 2004. Nonheme $Fe^{IV}O$ complexes that can oxidize the C-H bonds of cyclohexane at room temperature. J Am Chem Soc 126:472–473.

Kim J, Dong Y, Larka E, Que L, Jr. 1996. Electrospray ionization mass spectral characterization of transient iron species of bioinorganic relevance. Inorg Chem 35:2369–2372.

Kim C, Chen K, Kim J, Que L, Jr. 1997. Stereospecific alkane hydroxylation with H_2O_2 catalyzed by an iron(II)-*tris*(2-pyridylmethyl)amine complex. J Am Chem Soc 119:5964–5965.

Kobayashi T, Nishino S, Masuda H, Einaga H, Nishida Y. 2000. Detection of complex formation between binuclear iron(III)-peroxide adduct and oligonucleotide by electrospray mass spectrometry. Inorg Chem Commun 3:608–610.

Kochi JK, Siddall TL, Miyaura N, Huffman JC. 1983. Isolation and molecular structure of unusual oxochromium(V) cations for the catalytic epoxidation of alkenes. J Chem Soc Chem Commun 1185–1186.

Lau T-C, Wang J, Siu KWM, Guevremont R. 1994. Electrospray tandem mass spectrometry of oxo complexes of chromium, manganese and ruthenium. J Chem Commun 1487–1488.

McGarrigle EM, Gilheany DG. 2005. Chromium- and manganese-salen promoted epoxidation of alkenes. Chem Rev 105:1564–1602.

Messerschmidt A, Prade L, Wever R. 1997. Implications for the catalytic mechanism of the vanadium-containing enzyme chloroperoxidase from the fungus Curvularia inaequalis by X-ray structures of the native and peroxide form. Biol Chem 378:309–315.

Mialane P, Nivorojkine A, Pratviel G, Azema L, Slany M, Godde F, Simaan AJ, Banse F, Kargar-Grisel T, Bouchoux G, Sainton J, Horner O, Guilhem J, Tchertanova L, Meunier B, Girerd J-J. 1999. Structures of Fe(II) complexes with *N,N,N′-tris*(2-pyridylmethyl)-ethane-1,2-diamine type ligands. Bleomycin-like DNA cleavage and enhancement by an alkylammonium substituent on the N'atom of the ligand. Inorg Chem 38:1085–1092.

Molina-Svendsen H, Bojesen G, McKenzie CJ. 1998. Gas-phase reactivity of coordinatively unsaturated transition metal complex ions toward molecular oxygen. Inorg Chem 37:1981–1983.

Mouzopoulou B, Kozlowski H, Katsaros N, Garnier-Suillerot A. 2001. Structural characterization of Ru-bleomycin complexes by resonance raman, circular dichroism and NMR spectroscopy. Inorg Chem 40: 6923–6929.

Okutsu W, Ito S, Nishida Y. 1999. Electrospray mass spectrometry of the peroxide adduct of a monomeric Fe(III) complex containing a phenol group. Inorg Chem Commun 2:308–310.

Plattner DA. 2001. Electrospray mass spectrometry beyond analytical chemistry: Studies of organometallic catalysis in the gas phase. Int J Mass Spectrom 207:125–144.

Plattner DA. 2003. Metalorganic chemistry in the gas phase: Insight into catalysis. Top Curr Chem 225:153–203.

Plattner DA, Feichtinger D, El-Bahraoui J, Wiest O. 2000. Coordination chemistry of manganese-salen complexes studied by electrospray tandem mass spectrometry: The significance of axial ligands. Int J Mass Spectrom 195(196):351–362.

Que L, Jr., Tolman WB. 2002. Bis(μ-oxo)dimetal 'diamond' cores in copper and iron complexes relevant to biocatalysis. Angew Chem Int Ed 41:1114–1137.

Quiñonero D, Morokuma K, Musaev D, Mas-Ballesté R, Que L Jr. 2005. Metal-peroxo versus metal-oxo oxidants in non-heme iron-catalyzed olefin oxidations: Computational and experimental studies on the effect of water. J Am Chem Soc 127:6548–6549.

Rohde J-U, In J-H, Lim MH, Brennessel WW, Bukowski MR, Stubna A, Munck E, Nam W, Que L Jr. 2003. Crystallographic and spectroscopic characterization of nonheme Fe(IV)=O complex. Science 299:1037–1039.

Sam JW, Tang XJ, Peisach J. 1994. Electrospray mass spectrometry of iron bleomycin: Demonstration that activated bleomycin is a ferric peroxide complex. J Am Chem Soc 116:5250–5256.

Sam JW, Tang XJ, Magliozzo RS, Peisach J. 1995. Electrospray mass spectrometry of iron bleomycin II: Investigation of the reaction of Fe(III)- bleomycin with iodosylbenzene. J Am Chem Soc 117:1012–1018.

Shiren K, Ogo S, Fujinami S, Hayashi H, Suzuki M, Uehara A, Watanabe Y, Moro-oka Y. 2000. Synthesis, structures and properties of bis(μ-oxo)nickel(III) and *bis*(μ-superoxo)nickel(II) complexes: An unusual conversion of a $Ni_2^{III}(\mu\text{-}O)_2$ core into a $Ni_2^{II}(\mu\text{-}OO)_2$ core by H_2O_2 and oxygenation of ligand. J Am Chem Soc 122:254–262.

Simaan AJ, Banse F, Mialane P, Boussac A, Un S, Kargar-Grisel T, Bouchoux G, Girerd J-J. 1999. Characterization of nonheme mononuclear peroxoiron(III) intermediate by uv-vis and EPR spectroscopy and mass spectrometry. Eur J Inorg Chem 993–996.

Simaan AJ, Dopner S, Banse F, Bourcier S, Bouchoux G, Boussac A, Hildebrandt P, Girerd J-J. 2000. Fe^{III}-hydroperoxo and peroxo complexes with aminopyridyl ligands and the resonance raman spectroscopic identification of the Fe-O and O-O stretching modes. Eur J Inorg Chem 1627–1633.

Traeger JC. 2000. Electrospray mass spectrometry of organometallic compounds. Int J Mass Spectrom 200:387–401.

Traeger JC, Colton R. 1998. Electrospray ionization in inorganic chemistry. Adv Mass Spectrom Chapter 29:637–659.

Walanda DK, Burns RC, Lawrance GA, von Nagy-Felsobuki EI. 1999. New isopolyoxovanadate ions identified by electrospray mass spectrometry. Inorg Chem Commun 2:487–489.

Yamashita M, Fenn JB. 1984. Electrospray ion source. Another variation on the free-jet theme. J Phys Chem 88:4671–4675.

Zhang W, Loebach JL, Wilson SR, Jacobsen EN. 1990. Enantioselective epoxidation of unfunctionalized olefins catalyzed by (salen) manganese complexes. J Am Chem Soc 112:2801–2803.

Zheng H, Yoo SJ, Munck E, Que L Jr. 2000. The flexible $Fe_2(\mu\text{-}O)_2$ diamond core: A terminal iron(IV)-oxo species generated from the oxidation of a bis(μ-oxo)diiron(III) complex. J Am Chem Soc 122: 3789–3790.

Olga Bortolini received a Laurea degree with honours in Chemistry from the University of Padova (Italy) in 1979; Accademia dei Lincei research fellow at Padova University, 1980–1981. Researcher of the Italian National Research Council (CNR) since 1982. Post-doctoral research fellow at CNRS Laboratoire de Chimie de Coordination, Toulouse (France) in Prof. B. Meunier's group 1983. 1987–2003 Associate Professor of Organic Chemistry at the University of Ferrara. 2003 Full Professor of Organic Chemistry at the University of Calabria. June–August 1989, June–July 1992 and April–May 1994 Visiting Professor at Purdue University, West Lafayette IN, USA, in Prof. R.G. Cooks' group. Author of approximately 100 papers in international journals, many reviews, book chapters, and two patents.